Research Paper

Experimental validation of a flat punch indentation methodology calibrated against unconfined compression tests for determination of soft tissue biomechanics

R.M. Delaine-Smith[a,b,*], S. Burney[a], F.R. Balkwill[b], M.M. Knight[a]

[a]School of Engineering and Materials Science, Institute of Bioengineering, Queen Mary University of London, Mile End, London E1 4NS, UK

[b]Centre for Cancer and Inflammation, Barts Cancer Institute, Queen Mary University of London, Charterhouse Square, London EC1M 6BQ, UK

ARTICLE INFO

ABSTRACT

Mechanical characterisation of soft biological tissues using standard compression or tensile testing presents a significant challenge due to specimen geometrical irregularities, difficulties in cutting intact and appropriately sized test samples, and issues with slippage or damage at the grips. Indentation can overcome these problems but requires fitting a model to the resulting load–displacement data in order to calculate moduli. Despite the widespread use of this technique, few studies experimentally validate their chosen model or compensate for boundary effects. In this study, viscoelastic hydrogels of different concentrations and dimensions were used to calibrate an indentation technique performed at large specimen-strain deformation (20%) and analysed with a range of routinely used mathematical models. A rigid, flat-ended cylindrical indenter was applied to each specimen from which 'indentation moduli' and relaxation properties were calculated and compared against values obtained from unconfined compression. Only one indentation model showed good agreement ($<10\%$ difference) with all moduli values obtained from compression. A sample thickness to indenter diameter ratio $\geq 1{:}1$ and sample diameter to indenter diameter ratio $\geq 4{:}1$ was necessary to achieve the greatest accuracy. However, it is not always possible to use biological samples within these limits, therefore we developed a series of correction factors. The approach was validated using human diseased omentum and bovine articular cartilage resulting in mechanical properties closely matching compression values. We therefore present a widely useable indentation analysis method to allow more accurate calculation of material mechanics which is important in the study of soft tissue development, ageing, health and disease.

*Corresponding author at: School of Engineering and Materials Science, Queen Mary, University of London, Mile End Road, London E1 4NS, UK. Tel.: +44 20 7882 8770.
E-mail address: r.delaine-smith@qmul.ac.uk (R.M. Delaine-Smith).

1.   Introduction

Information describing the mechanical characteristics of biological tissues is important for a wide range of applications including understanding the activity and response of load-bearing tissues, measurement of pathological changes in diseased tissue for potential clinical diagnostics, determination of the cellular mechanical environment, or monitoring development of tissue engineered constructs. While there are many different techniques available for mechanically testing a wide range of materials, soft tissue characterisation presents a considerable challenge.

Two of the most widely used methods for determining mechanical properties of soft materials are compression and tensile testing. Compression involves deforming a plane-ended, typically cylindrical specimen with uniform cross-sectional area less than or equal to that of the compression platen, while tensile tests involve stretching the specimen held securely between two grips. Various different moduli may be calculated from the stress–strain curve generated from the load–displacement data normalised to sample dimensions. However, use of these techniques for soft biological tissues presents a significant challenge due to specimen geometrical irregularities and difficulties in cutting appropriately sized uniform test samples without causing damage. This means that there are few studies describing the compressive behaviour of soft tissues, especially those in the 1–100 kPa range e.g. adipose, breast, liver, kidney and prostate (Korhonen et al., 2002a; Shergold et al., 2006; Comley and Fleck, 2012). While uniaxial tensile testing of soft tissues is more common (Liu and Yeung, 2008; McKee et al., 2011; Screen et al., 2011; Alkhouli et al., 2013), due to the ability to better accommodate sample irregularities, difficulties can arise from sample slippage or damage at the grips.

To overcome the limitations of compressive and tensile testing, many studies use indentation which requires little or no sample preparation and results in minimal damage such that testing can even be performed in vivo or in situ (Mak, 1999; Then et al., 2012). Moduli values are determined by fitting a mathematical model to the resulting indentation load–displacement data. While compression data is independent of the platen size, indentation methods are highly dependent on indenter tip geometry and the relative dimensions of the indenter to the test specimen (Fischer-Cripps, 2000). Hemi-spherical indenters can minimize plastic deformation, stress concentrations and soft tissue damage but as with conical or pyramidal indenters, non-linear load–displacement responses occur as a result of increasing contact area making it harder to calculate modulus values. Use of a flat-ended cylindrical indenter simplifies theoretical analysis as the contact area is assumed to be constant throughout the loading period leaving only two mechanical variables, the contact force, $P(t)$, and the indenter displacement, $w(t)$, recorded as functions of time. Experimental measurement of these parameters allows for determination of the contact stiffness, S, which can then be used to calculated the elastic modulus.

Most soft tissues are known to display viscoelastic, anisotropic and non-linear responses to an externally applied mechanical force. However, as a first approximation many studies model tissues as linear, elastic, isotropic and incompressible in order to calculate modulus values. Simple mathematical models relate load and indentation depth while assuming infinitesimal strains and infinite sample thickness for linear elastic deformation (Sneddon, 1965; Johnson, 1985). To fulfil these conditions, the indentation depth must be small with respect to the indenter radius and the contact radius must be small with respect to the sample thickness and so in practice, the indentation depth to sample thickness ratio is commonly kept «10%. However, when complying with these assumptions it can be difficult to obtain useful indentation data from soft tissues, especially on relatively thin samples, due to their inherent low modulus values and potential surface irregularities, resulting in low signal-to-noise ratios. Therefore, large strain indentation is more favourable for soft tissue testing and solutions where simultaneous infringement of these assumptions occur have been modelled (Zhang et al., 1997).

While some investigators have implemented large indentation strains (>20%) on soft tissues including prostate and spleen (Carson et al., 2011; Umale et al., 2013), it has been shown that strains over 10% cause gross errors in modulus determination of brain tissue (Van Dommelen et al., 2010). Furthermore most simple mathematical models assume test samples to be semi-infinite media with no consideration for sample width or the relationship of sample width to thickness. This has led to few previous recommendations for ideal sample dimensions, namely that the sample should be at least 3–5 times the diameter of the indenter (Spilker et al., 1992; Krouskop et al., 1998; Egorov et al., 2008). A few studies have validated the chosen mathematical model experimentally but those that do tend to calibrate using samples that are non-representative of viscoelastic soft tissue (Samani et al., 2003; Egorov et al., 2008; Carson et al., 2011).

While tissue samples are usually non-uniform and heterogeneous, polymer hydrogels, such as agarose, can be cast to form plane ended uniform specimens with a range of dimensions and viscoelastic mechanical properties similar to that of soft tissues. Agarose forms homogenous compliant hydrogels with adjustable concentration-dependent mechanics and its mechanical behaviour has been well documented (Buckley et al., 2009). The viscoelastic nature of agarose hydrogels makes it an ideal candidate for use as a calibration material for mechanical characterization protocols and optimising testing methods for soft biological tissues.

The aim of this work was to test the suitability of an indentation technique with a range of simple mathematical models for the detailed characterisation of soft tissue viscoelastic mechanics using large strain deformation. This was achieved using agarose hydrogels of different concentrations (tangent modulus range 7–100 kPa) as calibration samples to compare the moduli and relaxation properties obtained by mathematical modelling of indentation data with those determined from unconfined compression (UC) tests. Further studies were conducted to examine the effect of specimen geometry which enabled the calculation of correction factors for specimens where an idealised geometry is not possible. Finally, the optimised test procedure was validated against compression testing using human diseased omental tissue

and bovine articular cartilage. The optimised methodology was able to generate moduli values with close agreement to those obtained by compression for both tissues. Thus we present a simple and widely useable methodology for calculating mechanical properties from indentation tests. We believe that this methodology has a wide range of applications particularly for testing of soft biological tissues.

2. Methods

2.1. Agarose gel preparation

Solutions of agarose (Type VII-A, low gelling temperature, Sigma, UK) were prepared at 0.75, 1, 1.5 and 2 w/v% in phosphate buffered saline (PBS) by melting at 90 °C and then mixing at 37 °C for 2 h. Uniform gels were cast in stainless steel moulds with dimensions 4 mm × 5 mm (height/thickness × diameter) for compressive samples and 2, 4 or 8 mm thick slabs for indentation samples. After 30 min at room temperature samples were transferred to 4 °C for a further 30 min. Temperature and cooling time were carefully controlled between batches since they are known to influence mechanical properties (Buckley et al., 2009). Samples were immediately removed from moulds and stored hydrated at 4 °C in PBS and tested within 48 h. For mechanical tests, compressive samples were tested at casted dimensions, while samples for indentation were cut to the required diameter with a cork borer. At least 6 samples from two batches of gels were tested for all experiments.

2.2. Compression and indentation testing of agarose

Mechanical characterisation was performed using a screw-driven MTS Synergie 100 (MTS Systems Corporation, USA), providing a cross-head position resolution of 1 μm, equipped with a ± 50 N load cell (resolution of 1 mN) and either a 7 mm diameter flat stainless steel platen for unconfined compression (UC) tests or a 4 mm diameter stainless steel flat-ended cylindrical probe for indentation tests. Hydrated samples were fully submerged in PBS at room temperature during testing. Schematics of both test setups are shown in Fig. 1a. Sample thickness was calculated by measuring the distance between the base of the sample dish and the top of the sample identified by an indenter load of 1 mN. For characterisation of agarose mechanics at different gel concentrations, samples were pre-loaded at 1 mN and then strained to 20% at a rate of 1% s^{-1} followed by a displacement-hold period of 360 s and then unloaded to 0% strain at a rate of 1% s^{-1}. Gels for indentation were 4 mm thick and 16 mm diameter. To test the effect of boundary conditions, 1.5 w/v% agarose gels were indented by varying the ratio of sample thickness (T_s) to
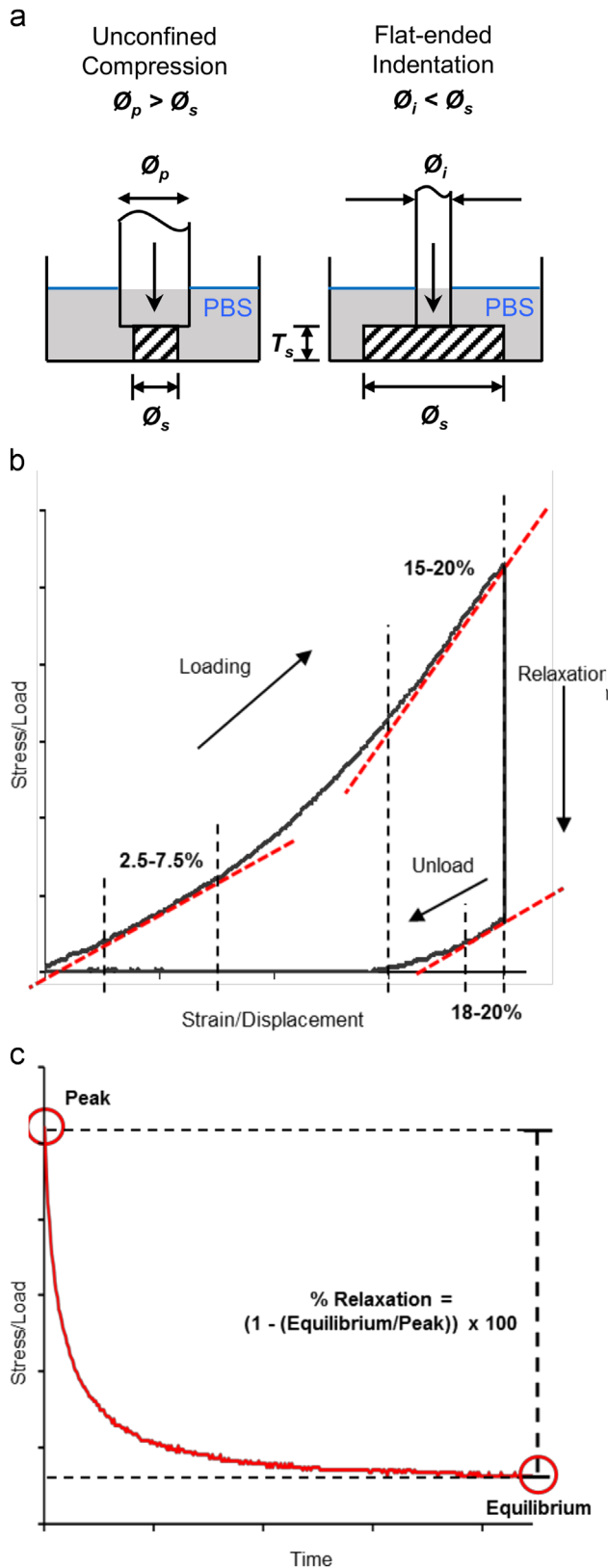
Fig. 1 – Schematics defining mechanical tests and characterization parameters. (a) Unconfined compression platen diameter ($Ø_p$) is greater than sample diameter ($Ø_s$) while flat-ended indenter diameter ($Ø_i$) is smaller than $Ø_s$, where T_s is specimen thickness after submersion in phosphate buffered saline (PBS). (b) Example test curve of stress/load-strain/displacement showing direction of loading, relaxation and unloading segments (indicated by arrows) and defined tangent moduli. (c) Example test curve of stress/load–time during relaxation phase indicating position of peak and equilibrium moduli, and calculation for % relaxation.

indenter diameter ($\emptyset_i$) (1:2, 1:1, 2:1) and by varying the ratio of sample diameter ($\emptyset_s$) to $\emptyset_i$ (2:1, 3:1, 4:1). To test for strain-rate effects, 1.5 w/v% agarose gels were tested at 3 different loading-strain rates $0.1\%\,s^{-1}$, $1\%\,s^{-1}$, or $10\%\,s^{-1}$.

2.3. Human omental tumour

Human diseased omentum was obtained from a patient undergoing surgical removal of tumorous tissue identified as high-grade serous ovarian cancer. Tissue samples were collected via the Research and Ethics Committee (REC) and Human Tissue Authority (HTA) approved Barts Gynae Tissue Bank (HTA license number 12199; REC no. 10/H0304/14). Tissue was transported in PBS and snap frozen to $-80\,°C$ where it was stored until use. Before testing, tissue was fully thawed to room temperature in PBS after which 4 mm cores were taken using a biopsy punch ($\sim$3 mm thick) for UC tests, with the rest of the tissue cut to size with a scalpel for indentation tests ($\sim$3 mm thick and $\geq$ 12 mm diameter). In this case, the stromal tumour regions were sufficiently stiff to enable a core specimen to be cut from the bulk tissue.

Mechanical characterisation of human omentum was performed using an Instron ElectroPuls E1000 (Instron, UK) equipped with a 10 N load cell (resolution of 0.1 mN) and either a 5 mm diameter flat stainless steel platen for UC tests or a 3 mm diameter stainless steel plane-ended cylindrical probe for indentation tests. Tissue-samples were submerged fully hydrated in PBS at room temperature throughout testing. For both UC and indentation, samples were pre-loaded to 0.5 mN and then loaded in an identical manner to that described for agarose with a max strain of 20% and a strain rate of $1\%\,s^{-1}$. After sufficient recovery time, samples were also strained to 30% using the same conditions with the exception of a hold period of 600 s at peak strain.

2.4. Bovine cartilage

Full depth cartilage explants were isolated from the proximal surface of bovine metacarpophalangeal joints of adult steers (18–24 months) using a 5 mm biopsy punch as in previous studies (Wann et al., 2010). Cored explants were snap frozen in PBS and stored at $-80\,°C$ until use. Before testing, explants were thawed to room temperature in PBS, samples were then divided for either compression tests, cored to 2 mm diameter discs, or kept at 5 mm diameter discs for indentation. A total of six non-matched explants were tested in compression and indentation.

Mechanical characterisation of bovine cartilage explants was performed using the MTS system with 50 N load cell and either a 3 mm diameter flat stainless steel platen for UC tests or a 1 mm diameter stainless steel plane-ended cylindrical probe for indentation tests. Cartilage explants were submerged fully hydrated in PBS at room temperature throughout testing. For both UC and indentation, samples were first pre-loaded to 5 mN and 3 mN respectively, and then loaded in an identical fashion as described for agarose and omental tumour but with a hold time at peak load of 600 s.

2.5. Analysis and mathematical models

The true compressive moduli for the agarose specimens were calculated directly from the stress–strain data. For indentation, the corresponding moduli were calculated from the load–displacement data with the aid of a mathematical model. Most indentation models determine the 'reduced' or 'effective' modulus, E^*, (Oliver and Pharr, 1992) defined as follows Eq. (2.1):

$$\frac{1}{E^*} = \frac{1-\nu_s^2}{E_s} + \frac{1-\nu_i^2}{E_i} \qquad (2.1)$$

In which E and ν are Young's modulus and Poisson's ratio respectively, while the subscripts s and i indicate specimen and indenter respectively. This takes into account elastic displacements that can occur in both sample and indenter, however, when the indenter is many orders of magnitude more rigid than the specimen (i.e steel versus soft tissue), contributions from the indenter become negligible.

The four mathematical models (M1–4) were selected based on either their wide spread use and/or previous application to soft tissue indentation (Hill, 1950; Timoshenko and Goodier, 1951; Sneddon, 1965; Hayes et al., 1972; Oliver and Pharr, 1992; Zhang et al., 1997; Krouskop, et al., 1998; Toyras et al., 1999; Korhonen et al., 2002a; Egorov et al., 2008; Carson et al., 2011). Models incorporating instantaneous displacement (w) and load (P) measurements are only suitable for linear elastic materials and so in each case the derivative, dP/dw, is used to take into account the nonlinearity of soft tissues allowing the indentation stiffness, S, to be calculated from any slope of the load–displacement curve. Table 1 shows that simplifying all models allows indentation modulus to be related to S and the indenter radius, a. A full explanation of model details can be found in Appendix A. Poisson's ratio for all samples was assumed to be 0.5. This is a reasonable assumption for all samples during instantaneous loading measurements when fluid flow out of the sample is minimal-low. During equilibrium measurements it is likely that Poisson's ratio will change for samples with significant fluid movement, but this is hard to calculate without direct measurements of sample size changes. All models assume isotropy in the samples and negligible friction.

Throughout the analysis, a series of well-established parameters were used as shown in Fig. 1b and c, including tangent moduli (TM) (2.5–7.5%; 15–20%; and unloaded 20–18%), peak modulus (PM) (end of loading phase/beginning relaxation phase) and equilibrium modulus (EQM) (end of relaxation phase). Peak modulus and equilibrium modulus were

Table 1 – Indentation mathematical models M1–4. E^*=reduced/effective modulus, E=indentation modulus, S=indentation stiffness, k=geometric correction factor, and a=indenter radius.

| Model	Modulus	References
M1	$E^* = S/2ak$	Hayes et al. (1972), Zhang et al. (1997)
M2	$E^* = S/2a$	Sneddon (1965), Oliver and Pharr (1992)
M3	$E^* = S/(\pi a/2)$	Hill (1950), Timoshenko and Goodier (1951), Krouskop et al. (1998)
M4	$E = S^*(3/\pi 2a)$	Timoshenko and Goodier (1951), Egorov et al. (2008)

calculated as the slope between zero load/displacement (indentation) or zero stress/strain (UC) and the load/displacement or stress/strain at peak or equilibrium respectively. A correction was applied to indentation unloading curves for agarose gels and cartilage explants to account for adhesion between the platen and the sample. This resulted in a small negative load during unloading followed by a sudden 'snap off' event to 0 N. The slope of the load–displacement plot in the negative load portion of the unloading phase was subtracted from the initial unloading slope. Both unloading moduli values are presented and termed unloading-1 (UNM-1) (not taking adhesion into account) and unloading-2 (UNM-2) (taking adhesion into account).

3. Results

3.1. Agarose concentration

All agarose gels showed a non-linear loading response and a high degree of stress–relaxation in both large strain UC and indentation confirming viscoelastic mechanical behaviour (Supplementary material 1). Increasing agarose gel concentration resulted in an increase in moduli but a slight reduction in the amount of relaxation. For the calculated parameters, the four indentation models were all able to distinguish between the different agarose concentrations. Fig. 2 shows plots of UC modulus versus indentation modulus for each model and the proximity with $y=x$ relationship such that the IN modulus perfectly predicts the UC modulus. M1 and M3 produced moduli values that were grossly lower ($\sim$50%) or higher ($\sim$30–70%) respectively than UC moduli, while M4 showed better agreement with UC values with generally less than 25% error. Overall, M2 produced values closest to UC moduli values (0–10% difference). Best fit lines were calculated (Table 2) from Fig. 2 showing that all models gave linear relationships ($y=mx+c$) with good correlation ($R^2 \geq 0.992$) between UC and indentation moduli. The linear correlations also confirmed that M2 produced values closest to UC values as shown by gradients close to 1. Flat ended cylindrical indentation of agarose showed a similar percentage relaxation compared with UC tested gels, however time
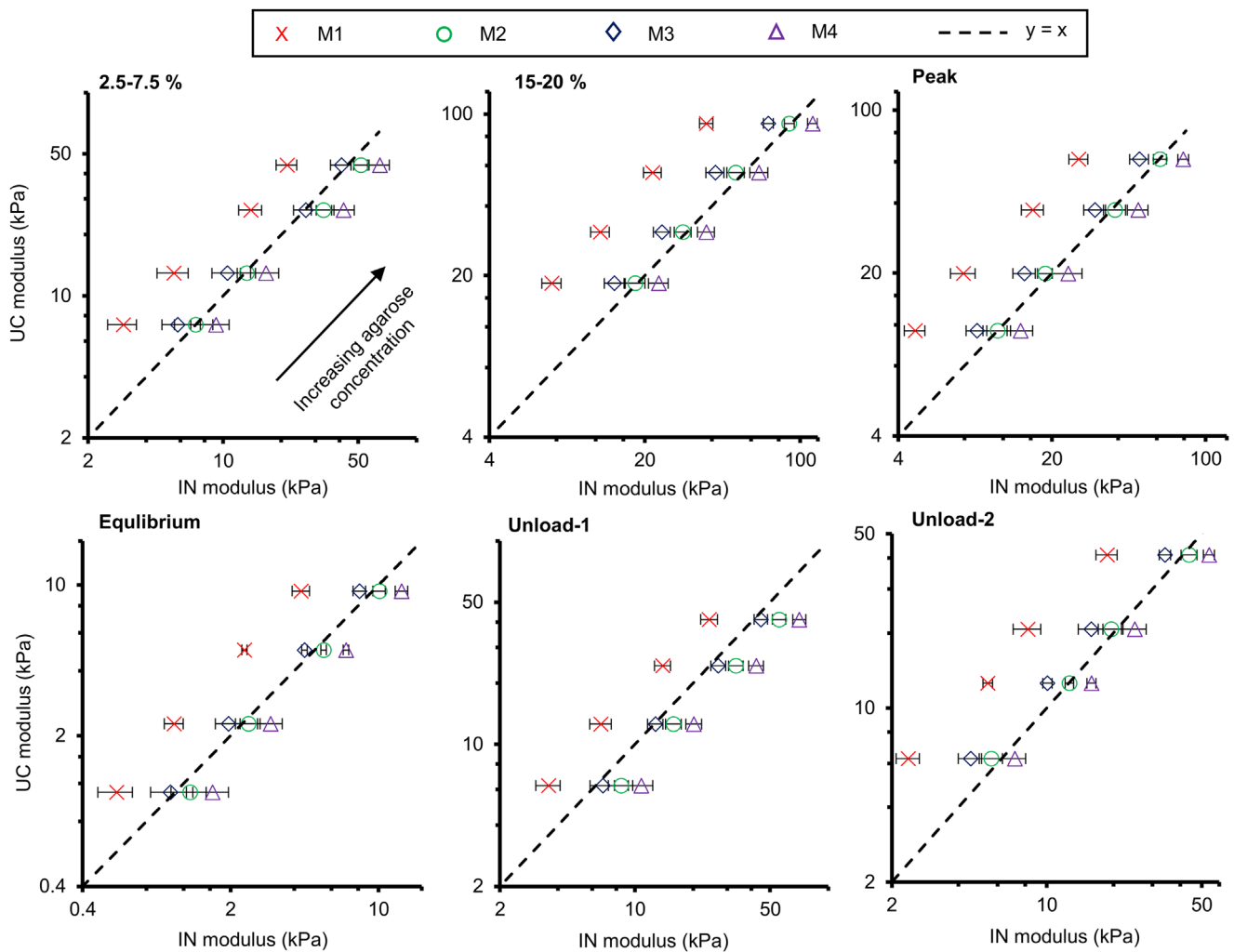
Fig. 2 – Unconfined compression (UC) moduli of agarose gels plotted against respective indentation (IN) moduli calculated using four mathematical models M1–4. Increasing agarose gel concentration (0.75, 1, 1.5 and 2 w/v%) resulted in increased moduli. Plotting experimental values of UC modulus against IN modulus visualizes the relationship that each model (M1–4) has with the true modulus represented by the dashed line ($y=x$). Scales are $\log_5$ plotting mean $\pm$ SD ($n \geq 6$).

Table 2 – Linear relationship derived from plots of compression moduli versus indentation moduli. Fig. 2 shows plots for different agarose gel concentrations (0.75, 1, 1.5 and 2 w/v%).

Model					Modulus							
	2.5–7.5%		15–20%		Peak		Equilibrium		Unload-1		Unload-2	
	R^2	Y	R^2	Y	R^2	Y	R^2	Y	R^2	Y	R^2	Y
M1	0.993	$1.96x+1.22$	0.997	$2.41x+1.05$	0.999	$2.27x+0.92$	0.999	$2.21x-0.16$	0.999	$1.66x+0.90$	0.995	$2.13x+1.66$
M2	0.995	$0.81x+1.37$	0.997	$1.02x+0.92$	0.998	$0.97x+0.74$	0.999	$0.94x-0.08$	0.999	$0.73x+0.40$	0.996	$0.91x+1.59$
M3	0.993	$0.65x+1.27$	0.997	$0.80x+0.94$	0.998	$0.76x+0.74$	0.999	$0.73x-0.08$	0.999	$0.57x+0.41$	0.998	$0.75x+1.16$
M4	0.992	$1.02x+1.27$	0.998	$1.27x+0.86$	0.998	$1.20x+0.72$	0.999	$1.16x-0.09$	0.999	$0.90x+0.39$	0.998	$1.18x+1.12$
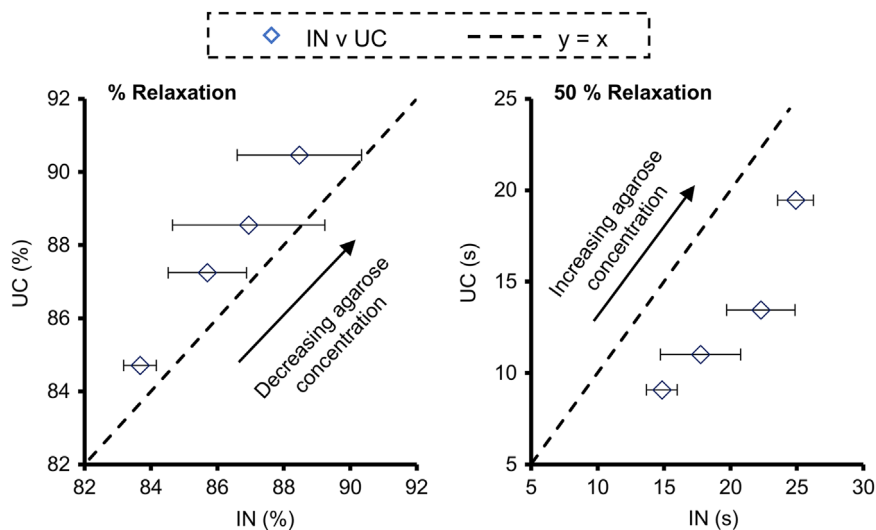
Fig. 3 – Relaxation properties of agarose gels obtained from unconfined compression (UC) and indentation (IN). Decreasing agarose gel concentration (0.75, 1, 1.5 and 2 w/v%) resulted in greater % relaxation and shorter time to 50% relaxation. Plotting UC versus IN relaxation properties obtained from experiments shows the relationship to the true relaxation properties represented by the dashed line ($y=x$). Data is mean $\pm$ SD ($n \geq 6$) where $y=1.19x-14.81$ ($R^2=0.999$) for % relaxation and $y=0.94x-5.53$ ($R^2=0.888$) for 50% relaxation.

for 50% relaxation took 75% longer for indentation (Fig. 3). In order to observe if specimen tests could be repeated to obtain identical load–displacement curves while using large strain indentation with a flat-ended cylinder, indentation tests were repeated on the same specimens at 0, 10 and 30 min after the initial test. After 0 and 10 min recovery, loading curves were different to the initial loading curve, however after 30 min recovery the loading curves were identical to the curve obtained from the initial test (Supplementary material 2).

3.2. Boundary effects—specimen geometry

Gels of 1.5 w/v% agarose with different dimensions were mechanically characterised via indentation (Fig. 4). Initial experiments showed that agarose specimens with a diameter $\geq 4:1$ ($\emptyset_s:\emptyset_i$) resulted in identical indentation load–displacement curves (results not shown). Changes in boundary conditions had relatively little effect on moduli values calculated with M1, regardless of the sample dimensions tested, M1 moduli values were always less than UC values and the % difference was generally 50–70%. All other models were affected by sample thickness. Thinner samples (decreased $T_s:\emptyset_i$) resulted in higher moduli values and therefore a higher

error% compared with UC. This was especially true for properties calculated after the relaxation period (EQM and UNM). Changes in $\emptyset_s$ had little effect on the moduli values calculated except for the 2.5–7.5% TM and UNM-2 values which showed a gradual increase and decrease respectively upon decreasing $\emptyset_s$, when $T_s:\emptyset_i$ was 1:2. Comparing relaxation properties between UC and indentation, both % relaxation and relaxation time to 50% were affected by T_s and $\emptyset_s$ (Fig. 5). To account for the differences in results obtained from compression tests and indentation M1 and M2, geometrical correction factors ($G\kappa$) were calculated (Table 3) in the form of a ratio representing the error% observed in Fig. 4.

The results described in Sections 3.1–3.2 indicated that the best agreement between moduli values obtained via UC and indentation were obtained using M2 when the following ideal specimen geometry was met $\emptyset_s:\emptyset_i \geq 4:1$ and $T_s:\emptyset_i \geq 1:1$ and $\leq 2:1$, generally requiring only a small correction. The linear correlations in Table 2 can be used to determine the corrected indentation modulus for specimens with the ideal specimen geometry by substitution of $E=x$. Where these conditions cannot be met ($\emptyset_s:\emptyset_i < 4:1$ and/or $T_s:\emptyset_i < 1:1$), $G\kappa$ can be applied by multiplication of calculated indentation moduli in order to obtain the corrected indentation modulus.
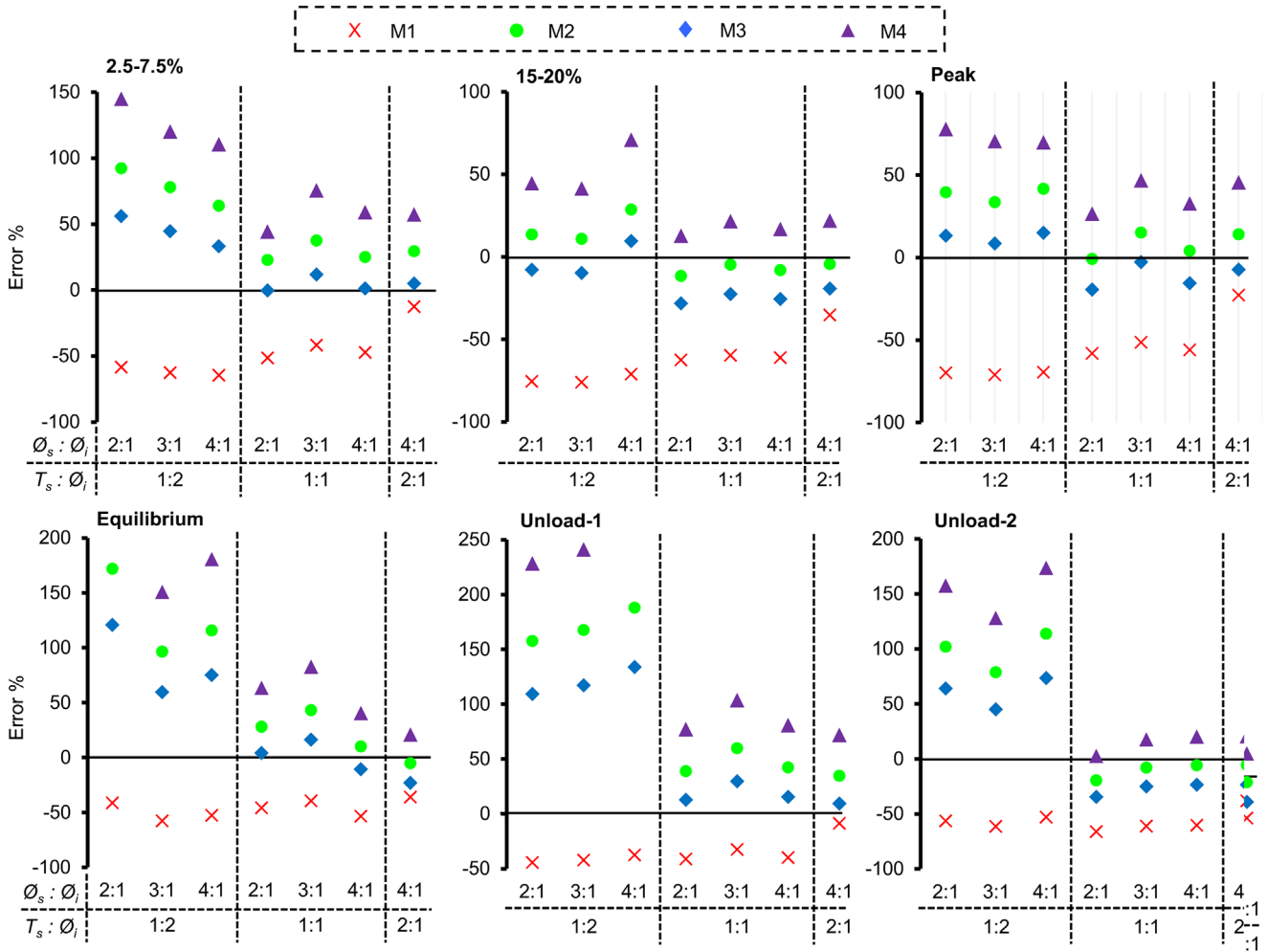
Fig. 4 – Error% resulting from difference between compression moduli and indentation moduli calculated using four mathematical models (M1–4) considering geometrical constraints. $\emptyset_s$ is sample diameter, $\emptyset_i$ is indenter diameter and T_s is sample thickness, numbers on x axis represents ratios of these. Data point for Unload-1 (M4) $\emptyset_s:\emptyset_i=4:1$ and $T_s:\emptyset_i=1:2$ is >250% and is not displayed. Data is mean ($n=6$).
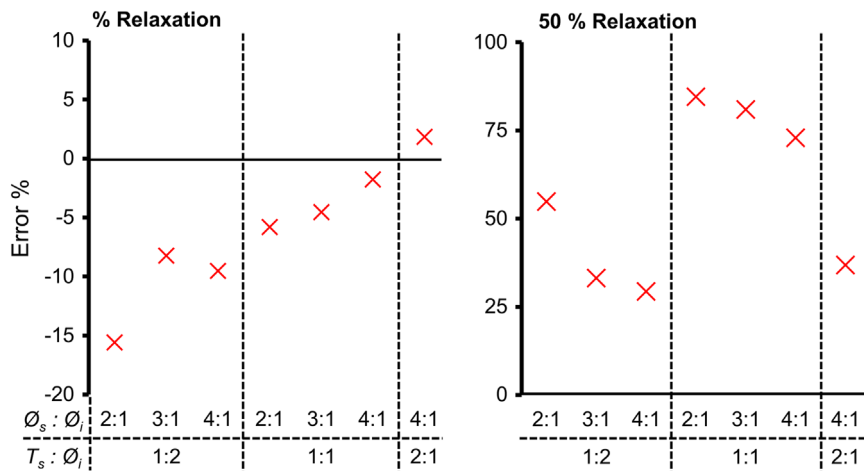
Fig. 5 – Error% resulting from difference between compression and indentation relaxation properties considering geometrical constraints. $\emptyset_s$ is sample diameter, $\emptyset_i$ is indenter diameter and T_s is sample thickness, numbers on x axis represents ratios of these. Data is mean ($n=6$).

Table 3 – Geometric correction factors ($G\kappa$) for flat-ended indentation. Correction factors were derived to account for differences between compression moduli and indentation (IN) moduli calculated using models M1–2 or relaxation properties between compression and indentation for different ratios of $\emptyset_s$ (sample diameter) and T_s (sample thickness) to $\emptyset_i$ (indenter diameter). Plots are displayed in Fig. 4.

Modulus	T_s: $\emptyset_i$	1:2			1:1			2:1
	$\emptyset_s$: $\emptyset_i$	2:1	3:1	4:1	2:1	3:1	4:1	4:1
2.5–7.5%	M1	2.41	1.96	2.83	2.06	1.72	1.90	1.14
	M2	0.52	0.56	0.61	0.81	0.73	0.80	0.77
15–20%	M1	4.08	4.18	3.46	2.68	2.48	2.58	1.54
	M2	0.88	0.90	0.78	1.13	1.05	1.09	1.05
Peak	M1	3.31	3.46	3.27	2.39	2.06	2.27	1.29
	M2	0.72	0.75	0.71	1	0.87	0.96	0.88
Equilibrium	M1	1.70	2.36	2.10	1.84	1.65	2.15	1.56
	M2	0.37	0.51	0.46	0.78	0.70	0.91	1.05
Unload	M1	1.80	1.73	1.60	1.70	1.48	1.67	1.10
	M2	0.39	0.37	0.35	0.72	0.63	0.70	0.74
Unload 2	M1	2.29	2.59	2.13	1.64	2.56	2.52	1.62
	M2	0.49	0.56	0.47	1.24	1.08	1.06	1.06
Relaxation %	IN	1.18	1.09	1.11	1.06	1.05	1.02	0.98
50% (Time)	IN	0.65	0.75	0.77	0.54	0.55	0.58	0.73

3.3. Strain-rate effects

Agarose gels (1.5 w/v%) were displaced to 20% strain at three different strain-rates across two orders of magnitude. All strain rates showed similar load-profiles up to 5% strain at which point the curves deviated in a strain-rate dependent manner (Supplementary material 3). Regardless of loading strain-rate, all samples showed relaxation to the same equilibrium point consistent with viscoelastic theory. Similarly, unloading profiles were almost identical for all samples. Having determined that M2 showed the best agreement with UC values at a strain rate of $1\% \, s^{-1}$ (Section 3.1), only this model was used for analysis of the effect of strain rate. Moduli for 2.5–7.5% TM, 15–20% TM and PM increased with increasing strain-rate and there was generally good agreement between indentation modulus values calculated with M2 and values calculated from UC (Fig. 6a). The EQM and UNM showed no dependence on loading strain-rate and indentation values closely matched UC values. Interestingly, when samples were loaded at the same strain-rate ($1\% \, s^{-1}$) and then unloaded at three different strain rates (0.1, 1 and $10\% \, s^{-1}$), there was no difference in the UNM between conditions (Supplementary material 4). At all 3 strain rates, % relaxation showed close agreement between indentation and UC as well as the time to 50% relaxation with the exception of the latter parameter at the highest strain rate (Fig. 6b). These results show that this indentation methodology is suitable for determination of strain-rate dependent effects.

3.4. Validation with human omental tumour

In order to examine the validity of the calibrated indentation procedure, we tested two different tissue types. Firstly we indented diseased omental tissue which showed a highly non-linear mechanical response when compressed or indented up to 20% strain followed by >85% stress/load relaxation (Fig. 7a). Consequently, tissue moduli increased 10-fold from the 2.5–7.5% TM to the 15–20% TM (Fig. 7b). Indentation data was used to calculate moduli values based on M1 and M2 and the corrected indentation modulus using M1 and incorporating the relevant G_κ value from Table 3 (T_s: $\emptyset_i$=1:1; $\emptyset_s$:$\emptyset_i$=4:1) termed M1-C. All moduli calculated using M2 showed good agreement with values obtained from UC tests. M1 values showed between 50% and 70% difference to UC values for all moduli (Fig. 7b), in a similar trend to that observed for agarose (Fig. 4). Calculation of the corrected indentation modulus using M1-C resulted in much closer agreement with UC values and values calculated using M2. Samples were also compressed or indented to 30% strain (Supplementary material 5) showing a 25–30% TM of ~250 kPa. As indentation of agarose was not performed at 30%, correction factors calculated for 20% strain were applied for M1-C. As with 20% strain tests, moduli calculated with M2 and M1-C showed good agreement with UC moduli. Relaxation properties were also similar between indentation and UC.

3.5. Validation with bovine cartilage

Bovine cartilage was analysed next to further test the suitability of the optimised indentation methodology. Indentation data was used to calculate moduli values based on M1 and M2, and the corrected models M1-C and M2-C. All explants had T_s:$\emptyset_i \leq 1$ with a range of thicknesses (0.6–1 mm) and this was taken into account using $G\kappa$ determined from Table 3. As all thickness measurements fell between T_s: $\emptyset_i$ 1:1–1:2, $G\kappa$ were calculated for each specimen from a linear curve fit of $G\kappa$ at T_s:$\emptyset_i$=1:1 and 1:2. Sample thickness was used to calculate individual κ values for M1 and M1-C. Cartilage specimens showed a non-linear loading profile and a large degree of relaxation at peak load (Fig. 8a). Generally, M1 underestimated mean moduli by 50–70% (Fig. 8b and c). By contrast, M2 overestimated all moduli. When both models were adjusted using the relevant $G\kappa$, moduli values showed substantially better agreement with UC values. The only exception was the 2.5–7.5% TM which was over estimated. The relaxation profile was very similar for UC and indentation (data not shown) and % relaxation also showed good agreement (<3% difference) (Fig. 8d). Overall, M1-C gave the best estimate of UC moduli values for these cartilage specimens. These results demonstrate the suitability of the indentation methodology for analysis of thin soft biological tissue where the ideal specimen geometry cannot be met.

4. Discussion

Indentation techniques and associated mathematical models used for the physical characterisation of soft tissue require experimental validation in order to obtain accurate and precise measurements. This study has identified a simple indentation methodology and a range of characterisation
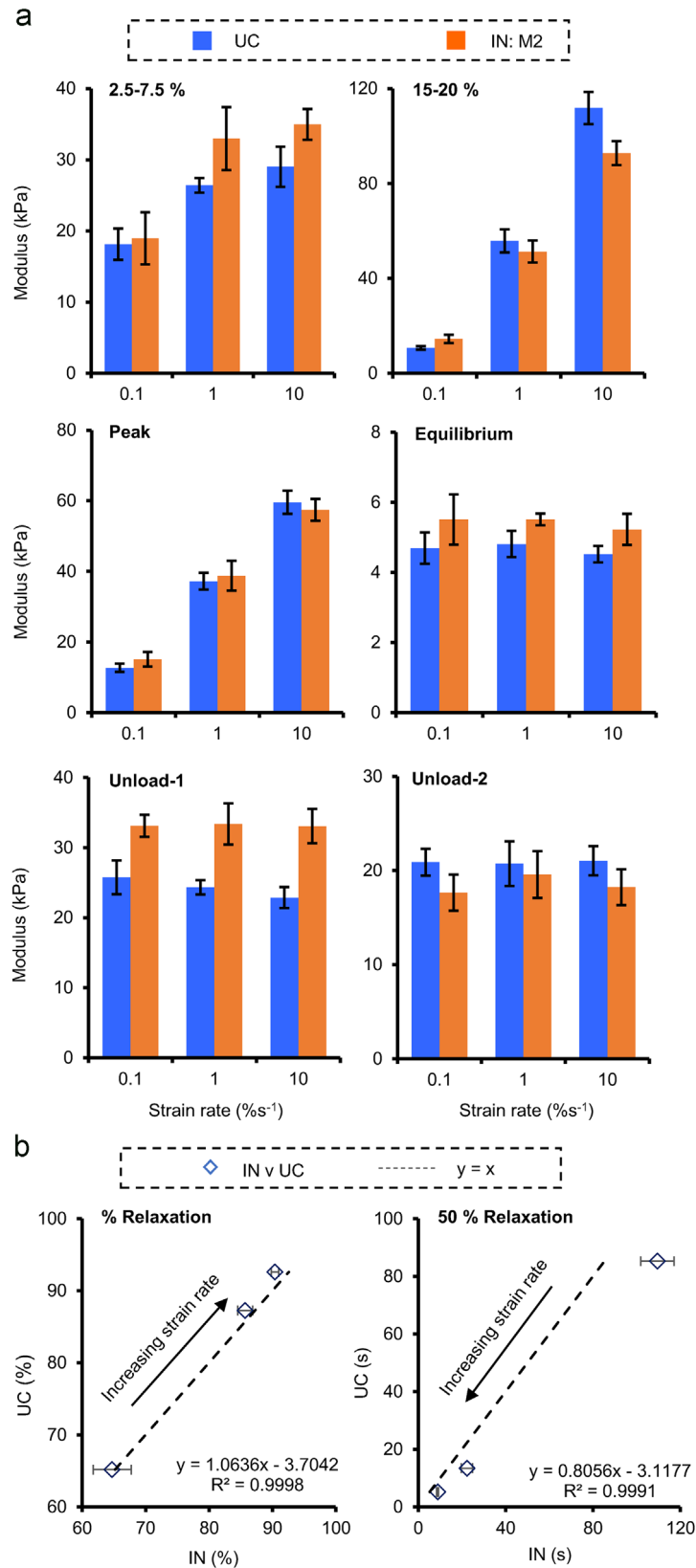
Fig. 6 – Moduli and relaxation properties obtained from compression and indentation of agarose at three different strain rates. Modulus values from UC and IN modulus calculated using M2 (a) plotted against load strain rate. Plotting UC versus IN relaxation properties obtained from experiments shows the relationship to the true relaxation properties represented by the dashed line ($y = x$). Data is mean $\pm$ SD ($n \geq 6$) where $y = 1.064x - 3.7$ ($R^2 = 0.999$) for % relaxation and $y = 0.81x - 3.12$ ($R^2 = 0.999$) for 50% relaxation.
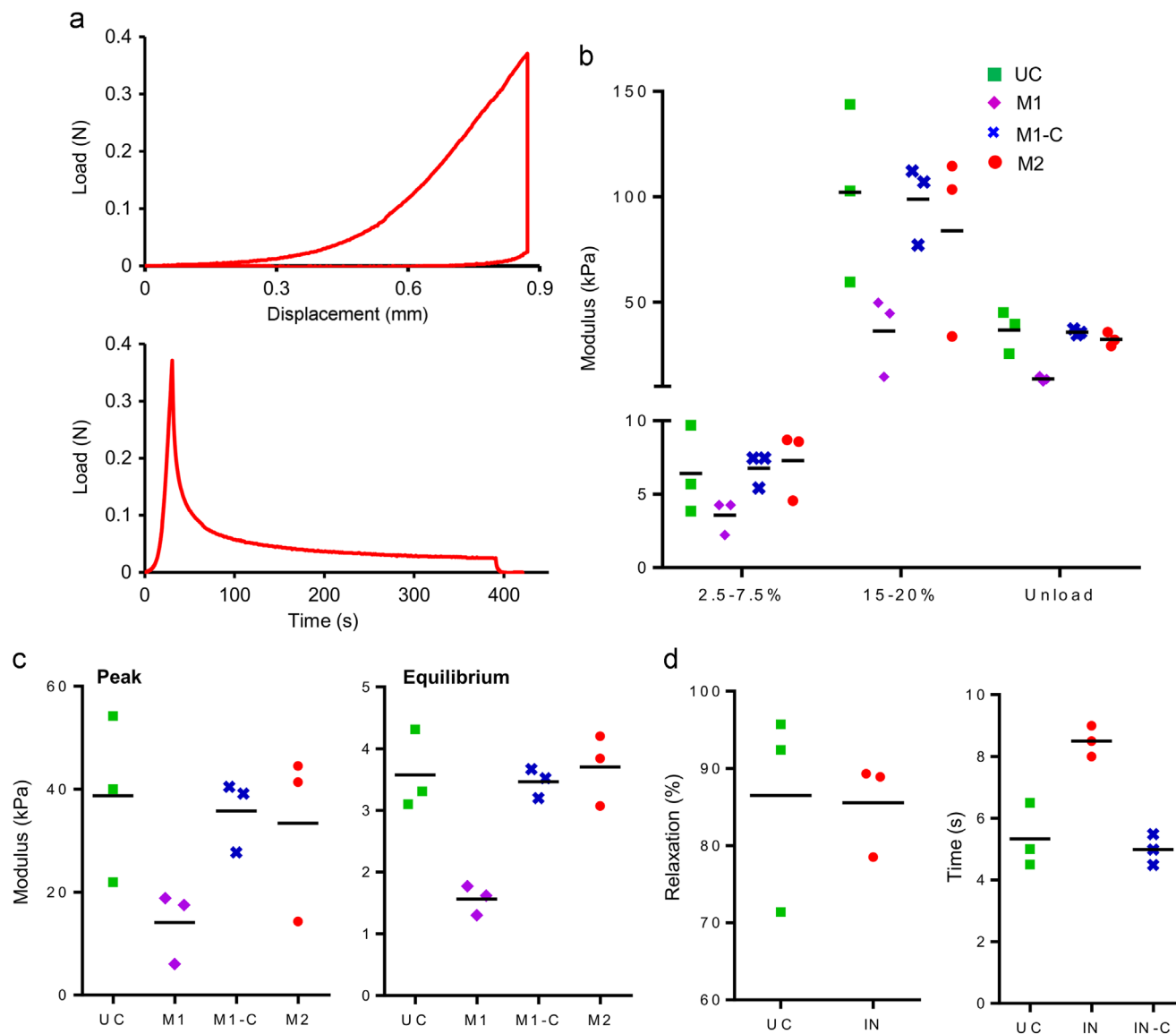
Fig. 7 – Representative indentation curves and individual plots of mechanical properties for human diseased omental tissue. Curves of load–displacement and load–time (a) show the entire loading-relaxation-unload test regime of diseased omental tissue, indicating non-linear and viscoelastic responses. Tangent moduli (b) and peak/equilibrium modulus (c) were plotted for individual specimens obtained from UC and indentation using models M1–2 and also M1 using the geometric correction value from Table S.2 (M1-C). IN-C used correction factor taken from Table S.2. Black lines represent the mean.

parameters that are suitable for the accurate measurement of ex vivo soft tissue biomechanics. Viscoelastic agarose hydrogels were used as calibration samples enabling calculation of correction factors for indentation models and geometric constraints. The optimised technique was further validated using two different soft biological tissues with a range of stiffness's (100 Pa–5 MPa).

In this study four simple mathematical models were tested in terms of their accuracy in producing values for mechanical parameters from large strain indentation tests that matched those obtained from unconfined compression. Soft tissues show non-linearity with increasing strain and exhibit viscoelastic properties and so cannot be described by a single modulus value. Thus a range of characterisation parameters were examined. Although complex methodologies exist to

calculate soft tissue mechanics (Then et al., 2012), simple indentation models provide a valuable and widely useable approach. To simplify analysis, researchers commonly assume large sample thickness and limit indentation depth («10%), but this limits the information obtainable from soft samples with inherently low modulus and or surface irregularities. It has been shown via finite element modelling that the classical solution is actually robust in accommodating large strain (Finan et al., 2014). In this study using large strain indentation experiments, M2 generally showed good agreement with compressive moduli for different agarose concentrations when the test specimen had the ideal specimen geometry. This model relates a constant indenter area, to the indentation stiffness, which can be derived from a slope on the load–displacement curve, generating a relatively good prediction of
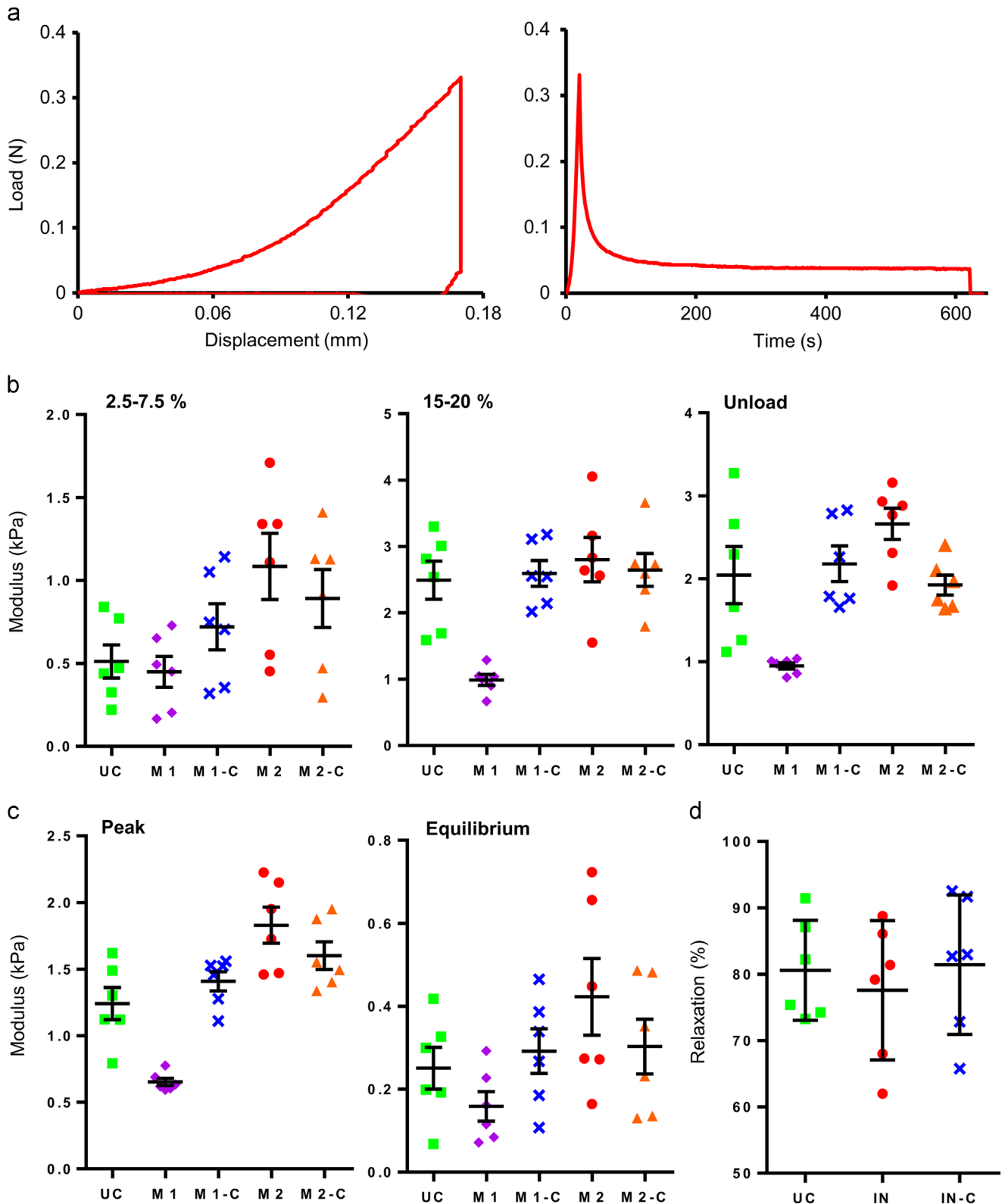
Fig. 8 – Representative indentation curves and individual plots of mechanical properties for bovine articular cartilage explants. Curves of load–displacement and load–time (a) show the entire loading-relaxation-unload test regime of cartilage explants, indicating non-linear and viscoelastic responses. Tangent moduli (b) and peak/equilibrium modulus (c) were plotted for individual specimens obtained from UC and indentation using models M1–2 and also corrected versions of M1 (M1-C) and M2 (M2-C) using the geometric correction factor from Table 3. IN-C used correction factor taken from Table 3. Black lines represent the mean±SEM.

E at any point on the curve. M1 was best able to adjust to specimens that were thinner than the ideal geometry, this is because the model accounts for the non-linear response of samples at different strains and ratios of $T_s:\emptyset_i$. This meant that the difference between $G\kappa$ ratios at different thicknesses was small. Therefore, specific $G\kappa$ values could be determined with good certainty from linear curve fitting of the $G\kappa$ values encompassing the test specimen geometry giving a good estimate of the corrected indentation modulus using M1.

In this study, all samples were treated as incompressible and assigned a Poisson's ration of $\nu = 0.5$. Although this is probably appropriate for the loading phase, it is likely that cartilage and agarose gels may have a Poisson's ratio of <0.5 during the relaxation phase due to fluid movement out of the sample. A wide range of ν values have been calculated for articular cartilage during both the instantaneous and equilibrium response, generally ranging from 0.1 to 0.5 (Korhonen et al., 2002a; Jin and Lewis, 2004; Kiviranta et al., 2006). However, Jin and Lewis (2004) calculated ν for bovine patellar cartilage during both the loading and relaxation phases of indentation showing it to be 0.5 and 0.46 respectively. Table 2 It has been shown that as tissue becomes thinner relative to the indenter diameter and as Poisson's ratio approaches 0.5, the effects of friction at the tissue–indenter interface become more significant (Spilker et al., 1992; Zhang et al., 1997). Finan et al. (2014) also stated that when the specimen becomes thinner and there is deviation from indentation of the infinite half space, the test closer resembles confined compression resulting in larger load as a result of limiting fluid movement out of the specimen. These reasons could explain why specimens with $T_s:\emptyset_i$ 1:2 showed the greatest moduli values.

Adhesion between the indenter surface and the specimen can result in an overestimation of the modulus (Carrillo et al., 2005; Johnson et al., 1971). Adhesion models are available to minimise adhesion effects on moduli (Johnson et al., 1971) which are often applied for AFM but less so in μm-scale indenting. Samples were kept hydrated and fully submerged in PBS throughout testing and it has been shown that full sample immersion can reduce or negate initial contact adhesion while reducing potential frictional effects. However, adhesion was observed in this study for both agarose and cartilage specimens and a simple correction was applied by subtracting the slope of negative load region of the unloading curve from the initial positive region. Omental tissue did not show any negative load and the initial indentation unloading slope matched well with the initial compressive unloading slope. Friction effects were ignored in all models, but they are assumed to be only of real significance during dynamic loading and less likely to affect quasi-static or equilibrium profiles as examined here.

Indentation stress is maximized at the point of indenter contact and diminishes radially away from this point. It is often recommended that indentation only be performed up to 10% strain to avoid underlying substrate effects (Bueckle, 1973). However, this is not a universal law and a number of parameters affect this including the indenter geometry, specimen thickness, adhesion, elastic and hardness properties of the sample/substrate, and strain rate (Chen and Vlassak, 2011; Julkunen et al., 2008). Consequently this rule is less likely to apply for testing soft tissues which are many

orders of magnitude softer than the underlying substrate. Increasing indentation strain rate effects the stress contours experienced within the sample such that the influence of the substrate increases as strain rate increases especially for a low $T_s:\emptyset_i$ ratio (Julkunen et al., 2008). The highest strain rate tested in this study did not appear to suffer from substrate effects, and so it would be up to future investigators to determine the maximum suitable strain rate for their samples. However, we would advise against performing large strain indentations (20%) on specimens with geometry $T_s:\emptyset_i > 2:1$ as the stresses created are likely to simulate a sharp point resulting in sample damage.

Normal omental tissue displays non-linear behaviour with tensile tangent moduli ranging from <3 kPa at 0–5% strain up to 30 kPa at 25–30% strain (Alkhouli et al., 2013) and it has been shown that adipose tissue has almost symmetrical tensile and compressive responses (Comley and Fleck, 2012). These results fit with the strain dependant indentation and compression moduli reported in this study. Human omental tissue used here was diseased and contained large regions of tumour, which was easily detected by both the compression tests and the indentation methodology with increasing TM from ~ 5 kPa (2.5–7.5%) up to 100 kPa (15–20%). Samples were also compressed or indented to 30% strain resulting in a 25–30% TM of ~ 250 kPa with good agreement between UC and the optimised indentation-models suggesting suitability of the optimised indentation method for strains up to 30%. Repeat loading of the omental specimen at increasing indentation strain after sufficient recovery (30 min) resulted in overlapping loading curves (Supplementary material 6), indicating minimal sample damage and showing the suitability of the methodology for progressive strain–relaxation tests.

Moduli values and relaxation properties calculated in this study from bovine articular cartilage tested in compression and indentation using corrected models, were in good agreement with other studies (Toyras et al., 1999; Jin and Lewis 2004; Irianto et al., 2014). However, a number of studies have found that indenting cartilage significantly over estimates elastic modulus values (Korhonen et al., 2002b; Julkunen et al., 2008). One possible reason is that the collagen fibrils organised tangentially in the superficial zone are strained in tension more effectively than with whole tissue compression (Korhonen et al., 2002a). This may explain the high 2.5–7.5% TM observed in this study compared with UC. Anisotropic effects observed in indentation is diminished relative to that seen in uniaxial tests on the same material oriented in the same manner; the multi-axial stress state under the indenter averages over the different stiffness directions to some extent. In another study, indentation of cell-laden collagen gels up to 30% showed no difference in the peak load between anisotropic and isotropic samples, but while relaxation behaviour was altered with isotropic specimens showing faster relaxation, samples eventually reached the same equilibrium point (Lake and Barocas 2012). In a previous study, M1 greatly overestimated bovine cartilage moduli in indentation versus UC by up to 107% (Julkunen et al., 2008), but under the conditions in this study it was shown to underestimate all moduli for agarose and cartilage explants by 50–70%. The error% for M1 was relatively unchanged for different $\emptyset_s:\emptyset_i$ or

T_s:$\varnothing_i$ ratios except when T_s:$\varnothing_i$=2:1 when it reduced to ~20%. By contrast all other methods were more sensitive to reductions in sample thickness. This is likely due to the κ values for M1 which already take into account the aspect ratio T_s:$\varnothing_i$ at different strain levels (Zhang et al., 1997), and may explain why analysis of cartilage explant indentation data with M1-C showed the best agreement with UC values.

The mathematical models used here allow calculation of the mechanical responses of soft viscoelastic materials under the applied experimental conditions at a given point in time. However, the models used in this study do not enable the calculation of viscoelastic components such as the viscosity (μ) and so cannot predict the full behaviour of viscoelastic materials. The models also do not allow prediction of poroelastic responses resulting from interstitial fluid movement during loading and relaxation. Empirical viscoelastic models consisting of springs and dashpots that represent elastic solid behaviour and viscous fluid behaviour respectively, can be used to better model viscoelastic behaviour. Higher-order models can be constructed such as the Maxwell–Wiechert model (Wang et al., 2013) by employing an increasing number of springs and dashpots. Models describing the contribution of poroelasticity and viscoelasticity have also been described (Strange et al., 2013) showing that relaxation is the product of both phenomena. The deformation process occurring in poroviscoelastic materials is complex and so often an array of models may be needed to describe a sample over magnitudes of strain rates. These multi-element models can greatly improve prediction of viscoelastic material behaviour, however, mathematical complexity is also increased.

These results demonstrate that the model and geometric correction factors calculated for soft agarose gels can also be applied to much stiffer (500x) viscoelastic tissue to give a more accurate measure of tissue moduli. Plotting the correlation of UC versus indentation moduli (M1 and M1-C) for agarose (6–90 kPa), human omentum (~250 kPa) and bovine cartilage explants (~2.5 MPa) together, yields a linear relationship over 4 orders of magnitude (Supplementary material 7) that can be used to closely estimate moduli values for tissues that fall within this range. This study highlights the importance of calibrating mechanical testing methodologies with suitable test specimens, especially for non-linear soft tissues, otherwise large errors can result depending on the chosen analytical model. The correction factors provided will now allow others to utilise simple indentation methodologies at large strains to provide more accurate mechanical properties. The following bullet point procedure is recommended for application of the correction method:

- Measure specimen diameter and thickness.
  - Ideal specimen geometry=$\varnothing_s$:$\varnothing_i \geq 4:1$, T_s:$\varnothing_i \geq 1:1$ and $\leq 2:1$.
- Perform indentation test and plot load–displacement curve to calculate S.
- For specimens: $\varnothing_s$:$\varnothing_i \geq 4:1$ and T_s:$\varnothing_i \geq 1:1$ calculate E using M2.
  - To correct: from Table 1 select corresponding Y=mx+c, where x=E.
- For specimens: $\varnothing_s$:$\varnothing_i < 4:1$ and/or T_s:$\varnothing_i < 1:1$ calculate E using M1.

- Calculate κ value (Zhang et al. 1997) using linear interpolation.
- To correct: Multiply E by Gκ derived from linear curve fitting of Gκ values encompassing test specimen dimensions in Table 3.

5. Conclusions

This study presents a simple flat-ended indentation methodology, with calibrated mathematical models, for improved calculation of a range of moduli and relaxation properties describing the mechanical characteristics of soft materials using large strains. Correction factors were developed to account for differences between properties derived from indentation load–displacement curves and compression stress–strain curves based on the chosen indentation model and sample geometry. Applying correction factors to indentation data for diseased-adipose tissue and thin articular cartilage explants enabled calculation of mechanical properties closely matching those obtained from compression tests. When $\varnothing_s$:$\varnothing_i \geq 4:1$ and T_s:$\varnothing_i \geq 1:1$, M2 produced the smallest error% and so is recommended for use with specimens meeting these ideal geometric conditions. M1 one was best able to account for reductions in sample thickness and so is recommended for specimens when T_s:$\varnothing_i \leq 1:1$. The presented methodology is also suitable for characterisation of relaxation properties and strain rate effects. We believe that the calibrated and validated indentation methodology is widely accessible and will benefit researchers interested in mechanical characterisation of materials within the 1 kPa–10 MPa range making it particularly suitable for soft biological tissues.

Acknowledgements

Appendix A. Mathematical models

A.1. Model 1

Hayes et al. (1972) derived a geometric correction factor (κ) from axisymmetric flat-ended indentation of cartilage, modelled as an elastic layer fixed to a rigid boundary, to take sample thickness into consideration. This enabled calculation of the elastic modulus as shown in Eq. (A.1):

$$E = \frac{P(1-v^2)}{2awk} \tag{A.1}$$

Hayes' solution assumes infinitesimal deformation ($\leq 0.1\%$ strain), infinite sample thickness and linear theory, however indentation tests using large displacements ($\geq 10\%$

strain) make the solution unsuitable for non-linear tissue samples. To account for non-linearity, Eq. (A.1) can be expressed as Eqs. (A.2) or (A.3) (Toyras et al., 1999; Korhonen et al., 2002a)

$$E = E_{measured}\left(\frac{\pi a}{2h\kappa}\left(1 - v^2\right)\right) \tag{A.2}$$

$$E = \frac{\left(1 - v^2\right)}{2a\kappa} \times \frac{dP}{dw} \tag{A.3}$$

whereby $E_{measured}$ is the slope of the indentation stress versus strain curve, $d(P/\pi a^2)/d(w/h)$, and h is sample thickness. These solutions simplify to the following Eq. (A.4), hereby termed model 1 (M1).

$$E^* = S/2a\kappa \tag{A.4}$$

Zhang et al. (1997) provided new κ factors to account for large deformation non-linear behaviour. They state that κ values are approximately proportional to indentation strain and that linear interpolation of their data can be used to obtain values at larger strains. These κ factors are used for M1.

A.2.   Model 2

The solution of Sneddon (1965) for the axisymmetric Boussinesq problem has been widely popularised by Oliver and Pharr (1992) who showed that the elastic contact stiffness, S, is related to the contact area, $A = \pi a^2$, and the effective elastic modulus, E^*, via the following relationship given in equation (A.5).

$$E^* = \frac{1}{\beta} \times \frac{dP}{dw} \times \frac{1}{2} \times \frac{\sqrt{\pi}}{\sqrt{A}} \tag{A.5}$$

Where β is a constant such that $\beta = 1$ for flat-ended indenter and hence Eq. (A.5) simplifies to Eq. (A.6) and termed model 2 (M2).

$$E^* = S/2a \tag{A.6}$$

This technique was originally used to characterise hard materials, mainly in thin sheet form, but has also been used to characterise indentation unloading slopes of ex vivo prostate tissue (Carson et al., 2011). It is described as being insensitive to indenter diameter and sample thickness. This model is routinely applied to the initial slope of the unloading load–displacement curve and is rarely applied in the calculation of other moduli values.

A.3.   Model 3

Krouskop et al. (1998) used the following solution for the flat-ended indentation of normal and diseased breast tissue describing a uniform load acting over part of the boundary of a semi-infinite elastic solid (Timoshenko and Goodier, 1951) Eq. (A.7).

$$E = \frac{2(1 - v^2)qa}{w} \tag{A.7}$$

Where q is the load density or indentation stress. Eq. (A.7) is also equivalent to the nominal indentation stress-indentation strain relationship for a flat ended indenter (Hill, 1950) Eq. (A.8).

$$E^* = \frac{P}{\pi a^2} \div \frac{w}{2a} \tag{A.8}$$

Taking the differential of Eq. (6.8) and simplifying to Eq. (6.9) gives model 3 (M3).

$$E^* = \frac{S}{(\pi a/2)} \tag{A.9}$$

Krouskop et al. (1998) claimed that indentation of uniform cylindrical gels produced elastic modulus values that showed less than 5% difference to values calculated using UC. While this model assumes the indentation response to be free of substrate effects, Krouskop et al. recommended using $\varnothing_s{:}T_s$ ratio $\geq 4{:}1$ and a $\varnothing_s{:}\varnothing_i$ ratio $\geq 4{:}1$.

A.4.   Model 4

Egorov et al. (2008) indented a range of soft tissues using a model for semi-infinite media (Timoshenko and Goodier, 1951) which ignores the effects of boundary conditions (A.10), this is model 4 (M4).

$$E = \frac{3}{\pi^2 a} \times \frac{dP}{dw} = \frac{3}{\pi^2 a}S \tag{A.10}$$

Egorov et al. (2008) stated that sample dimensions had to follow $T_s{:}\varnothing_i$ ratio $\geq 2{:}1$ and a $\varnothing_s{:}\varnothing_i$ ratio $\geq 3{:}1$ so that the semi-infinite media model was applicable for calculating Young's modulus. The model is also independent of Poisson's ratio.

Appendix B.   Supplementary material

Supplementary data associated with this article can be found in the online version at http://dx.doi.org/10.1016/j.jmbbm.2016.02.019.

REFERENCES

Alkhouli, N., Mansfield, J., Green, E., et al., 2013. The mechanical properties of human adipose tissues and their relationships to the structure and composition of the extracellular matrix. Am. J. Physiol. Endocrinol. Metab. 305, E1427–E1435, http://dx.doi.org/10.1152/ajpendo.00111.2013.

Buckley, C.T., Thorpe, S.D., O'Brien, F.J., et al., 2009. The effect of concentration, thermal history and cell seeding density on the initial mechanical properties of agarose hydrogels. J. Mech. Behav. Biomed. Mater. 2, 512–521, http://dx.doi.org/10.1016/j.jmbbm.2008.12.007.

Bueckle, H., 1973. The Science of Hardness Testing and its Research Applications. American Society for Metals, Ohio.

Carrillo, F., Gupta, S., Balooch, M., et al., 2005. Nanoindentation of polydimethylsiloxane elastomers: effect of crosslinking, work of adhesion, and fluid environment on elastic modulus. J. Mater. Res. 10, 2820–2830.

Carson, W.C., Gerling, G.J., Krupski, T.L., et al., 2011. Material characterization of ex vivo prostate tissue via spherical indentation in the clinic. Med. Eng. Phys. 33, 302–309, http://dx.doi.org/10.1016/j.medengphy.2010.10.013.

Chen, X., Vlassak, J.J., 2011. Numerical study on the measurement of thin film mechanical properties by means of nanoindentation. J. Mater. Res. 16, 2974–2982, http://dx.doi.org/10.1557/JMR.2001.0408.

Comley, K., Fleck, N., 2012. The compressive response of porcine adipose tissue from low to high strain rate. Int. J. Impact Eng. 46, 1–10, http://dx.doi.org/10.1016/j.ijimpeng.2011.12.009.

Egorov, V., Tsyuryupa, S., Kanilo, S., et al., 2008. Soft tissue elastometer. Med. Eng. Phys. 30, 206–212, http://dx.doi.org/10.1016/j.medengphy.2007.02.007.

Finan, J.D., Fox, P.M., Morrison, B., 2014. Non-ideal effects in indentation testing of soft tissues. Biomech. Model Mechanobiol. 13, 573–584, http://dx.doi.org/10.1007/s10237-013-0519-7.

Fischer-Cripps, A.C., 2000. A review of analysis methods for submicron indentation testing. Vacuum 58, 569–585, http://dx.doi.org/10.1016/S0042-207X(00)00377-8.

Hayes, W.C., Keer, L.M., Herrmann, G., Mockros, L.F., 1972. A mathematical analysis for indentation tests of articular cartilage. J. Biomech. 5, 541–551, http://dx.doi.org/10.1016/0021-9290(72)90010-3.

Hill, R., 1950. The Mathematical Theory of Plasticity. Oxford University Press.

Irianto, J., Ramaswamy, G., Serra, R., Knight, M.M., 2014. Depletion of chondrocyte primary cilia reduces the compressive modulus of articular cartilage. J. Biomech. 47, 579–582, http://dx.doi.org/10.1016/j.jbiomech.2013.11.040.

Jin, H., Lewis, J.L., 2004. Determination of Poisson's ratio of articular cartilage by indentation using different-sized indenters. J. Biomech. Eng. 126, 138–145, http://dx.doi.org/10.1115/1.1688772.

Johnson, K.L., 1985. Contact Mechanics. Cambridge University Press.

Johnson, K.L., Kendall, K., Roberts, A.D., 1971. Surface energy and the contact of elastic solids. Proc. R. Soc. A Math. Phys. Eng. Sci. 324, 301–313.

Julkunen, P., Korhonen, R.K., Herzog, W., Jurvelin, J.S., 2008. Uncertainties in indentation testing of articular cartilage: a fibril-reinforced poroviscoelastic study. Med. Eng. Phys. 30, 506–515, http://dx.doi.org/10.1016/j.medengphy.2007.05.012.

Kiviranta, P., Rieppo, J., Korhonen, R.K., et al., 2006. Collagen network primarily controls Poisson's ratio of bovine articular cartilage in compression. J. Orthop. Res. 24, 690–699, http://dx.doi.org/10.1002/jor.

Korhonen, R.K., Laasanen, M.S., Töyräs, J., et al., 2002a. Comparison of the equilibrium response of articular cartilage in unconfined compression, confined compression and indentation. J. Biomech. 35, 903–909, http://dx.doi.org/10.1016/S0021-9290(02)00052-0.

Korhonen, R.K., Wong, M., Arokoski, J., et al., 2002b. Importance of the superficial tissue layer for the indentation stiffness of articular cartilage. Med. Eng. Phys. 24, 99–108, http://dx.doi.org/10.1016/S1350-4533(01)00123-0.

Krouskop, T.A., Wheeler, T.M., Kallel, F., et al., 1998. Elastic moduli of breast and prostate tissues under compression. Ultrason. Imaging 20, 260–274, http://dx.doi.org/10.1177/016173469802000403.

Lake, S.P., Barocas, V.H., 2012. Mechanics and kinematics of soft tissue under indentation are determined by the degree of inital collagen fiber alignment. J. Mech. Behav. Biomed. Mater 13, 25–35.

Liu, Z., Yeung, K., 2008. The preconditioning and stress relaxation of dkin tissue. J. Biomed. Pharm. Eng. 1, 22–28, http://dx.doi.org/10.1007/s00238-011-0671-1.

Mak, A.F.T., 1999. Effective elastic properties for lower limb soft tissues from manual indentation experiment. IEEE Trans. Rehabil. Eng. 7, 257–267, http://dx.doi.org/10.1109/86.788463.

McKee, C.T., Last, J.A., Russell, P., Murphy, C.J., 2011. Indentation versus tensile measurements of Young's modulus for soft biological tissues. Tissue Eng. Part B Rev. 17, 155–164, http://dx.doi.org/10.1089/ten.teb.2010.0520.

Oliver, W.C., Pharr, G.M., 1992. An improved technique for determining hardness and elastic modulus using load and displacement sensing indentation experiments. J. Mater. Res. 7, 1564–1583.

Samani, A., Bishop, J., Luginbuhl, C., Plewes, D.B., 2003. Measuring the elastic modulus of small tissue samples. Phys. Med. Biol. 48, 2183–2198, http://dx.doi.org/10.1177/016173469802000102.

Screen, H.R.C., Seto, J., Krauss, S., et al., 2011. Extrafibrillar diffusion and intrafibrillar swelling at the nanoscale are associated with stress relaxation in the soft collagenous matrix tissue of tendons. Soft Matter 7, 11243, http://dx.doi.org/10.1039/c1sm05656e.

Shergold, O.A., Fleck, N.A., Radford, D., 2006. The uniaxial stress versus strain response of pig skin and silicone rubber at low and high strain rates. Int. J. Impact Eng. 32, 1384–1402, http://dx.doi.org/10.1016/j.ijimpeng.2004.11.010.

Sneddon, I.N., 1965. The relation between load and penetration in the axisymmetric Boussinesq problem for a punch of arbitrary profile. Int. J. Eng. Sci. 3, 47–57, http://dx.doi.org/10.1016/0020-7225(65)90019-4.

Spilker, R.L., Suh, J.K., Mow, V.C., 1992. A finite element analysis of the indentation stress–relaxation response of linear biphasic articular cartilage. J. Biomech. Eng. 114, 191–201.

Strange, D.G.T., Fletcher, T.L., Tonsomboon, K., et al., 2013. Separating poroviscoelastic deformation mechanisms in hydrogels. Appl. Phys. Lett. 102, 031913.

Then, C., Vogl, T.J., Silber, G., 2012. Method for characterizing viscoelasticity of human gluteal tissue. J. Biomech. 45, 1252–1258, http://dx.doi.org/10.1016/j.jbiomech.2012.01.037.

Timoshenko, S., Goodier, J.N., 1951. Theory of Elasticity, 2nd ed. McGraw-Hill Book Company.

Toyras, J., Rieppo, J., Nieminen, M., et al., 1999. Characterization of enzymatically induced degradation of articular cartilage using high frequency ultrasound characterization of enzymatically induced degradation of articular cartilage using high frequency ultrasound. Phys. Med. Biol. 44, 2723–2733.

Umale, S., Deck, C., Bourdet, N., et al., 2013. Experimental mechanical characterization of abdominal organs: liver, kidney & spleen. J. Mech. Behav. Biomed. Mater. 17, 22–33, http://dx.doi.org/10.1016/j.jmbbm.2012.07.010.

Van Dommelen, J.A.W., van der Sande, T.P.J., Hrapko, M., Peters, G.W.M., 2010. Mechanical properties of brain tissue by indentation: interregional variation. J. Mech. Behav. Biomed. Mater. 3, 158–166, http://dx.doi.org/10.1016/j.jmbbm.2009.09.001.

Wang, X., Schoen, J.A., Rentschler, M.E., 2013. A quantitative compariosn of soft tissue compressive viscoelastic model accuracy. J. Mech. Behav. Biomed. Mater. 20, 126–136.

Wann, A.K.T., Mistry, J., Blain, E.J., et al., 2010. Eicosapentaenoic acid and docosahexaenoic acid reduce interleukin-1β-mediated cartilage degradation. Arthritis Res. Ther. 12, R207, http://dx.doi.org/10.1186/ar3183.

Zhang, M., Zheng, Y.P., Mak, A.F.T., 1997. Estimating the effective Young's modulus of soft tissues from indentation tests—nonlinear finite element analysis of effects of friction and large deformation. Med. Eng. Phys. 19, 512–517, http://dx.doi.org/10.1016/S1350-4533(97)00017-9.